Research Journal of Optics and Photonics

Review Article

A SCITECHNOL JOURNAL

Fully Integrated Large Arrays of 3D Microtubular Ring Resonators with Polymer Waveguides

Abbas Madani*

Institute for Integrative Nanosciences, Cambridge Graphene Centre, University of Cambridge, Black Semiconductor GmbH,Otto-Blumenthal-Strasse Germany

Abstract

A novel platform for optofluidic applications is realized by monolithic integration of an array of ultra-compact three-dimensional (3D) vertically rolled-up microtube ring resonators (VRU- MRRs) with polymer waveguides. The on-chip integrated system is realized by rolling up 2D differentially strained TiO2 nanomembranes into 3D microtubular cavities on a nanophotonic chip and seamlessly overlaid over several integrated waveguides. Whispering-gallery modes are observed in the telecom wavelength range, and their spectral peak positions shift significantly when measurements are performed while immersing the tubes or filling their hollow cores with water, thus manifesting a compact, robust all-integrated optofluidic microtube ring resonator with a high functionality, and well suited for dense multiplexing of sensors. In this intriguing vertical transmission scheme, optical characterization of the air filled integrated VRU-MRRs reveals an extinction ratio as high as 32 dB, which is the highest, recorded for an integrated VRU- MRR to date. In the case of solution-filled VRU-MRR, the maximum extinction ratio of this integrated system is as high as 10 dB due to the strong absorption of water at telecom wavelengths. Thus, this change in the transmission spectrum of the VRU-MRRs represents a novel sensing methodology in addition to using spectral mode shifts. The achievement of this work opens up fascinating opportunities to realize massively parallel optofluidic microsystems with exceptional multi-functionality and flexibility for analysis of biomaterials in lab-in-a-tube systems on a single chip.

Keywords: Optofluidic; Microtubular; Microresonators; Nanophotonic; Polymer waveguides.

Introduction

QOptofluidics isan emerging research area in which micro/nano fluidics are unified with integrated optical components on the same platform [1]. Optofluidics has held the great promise for creating modern devices to use them in many applied systems that deal with liquid analytes [2]. But thus for only a few devices have been successfully marketed. To date, whispering-gallery-mode (WGM) microresonators have proved to be an excellent choice for optofluidic sensing applications, owing to their ability to traplight in small volumes for long periods of time via TIR [2-5]. Among these devices, liquid core optical ring resonators (LCORRs are particularly interesting because they possess inherent hollow cores, which naturally offer built-in microfluidic channels for optofluidic applications [8,9]. More importantly, because of the micrometer-sized such resonators, only (sub-) picoliter volumes of diverse analytes are required, which might be considered as an indispensable asset for potential microfluidic applications. In general, the LCORRs are often fabricated by heating-and-pulling glass capillaries, which is however not suitable for on-chip integration owing to the fabrication method, structure fragility and large sizes. From other hand, an off-chip tapered fiber scheme is usually used to send light in and out of these resonators. Hence, four factors can be hampered the widespread use of such systems in optofluidic sensing applications and also in many other applications. First, these systems are delicate and difficult to handle. Second, these systems are fragile and quite unstable. Third, the portability of such systems is quite poor. Fourth, the off-chip tapered fibers are not integrated with the microresonators although this is one of the important requirements of integrated optofluidic applications. Thus, apart from the sensitivity of these systems, the fully integration of these resonators on a photonic chip is a very important aspect for optofluidic sensors.

As discussed in the previous sections, rolled-up nanotech is recognized as an efficient approach to create vertically rolled-up ring resonators (VRU-MRRs) with controllable shape and size, which is compatible with on-chip integration and can be a promising solution to satisfy these aforementioned demands [28,29]. In addition to this and unlike the LCORRs and other resonators (i.e., microspheres, microtoroids, microrings, microdisks, etc.) VRU-MRRs represent excellent optical confinement and a high degree of mechanical stability, and they are well-suited for use in integrated microfluidic channels [32,33,].

Their unique properties are discussed in detail in to date, the optofluidic applications of the isolated VRU-MRRs (i.e. microtubes that are not coupled with optical waveguides) have been demonstrated by inserting a liquid core into a free-standing tube [32] or a tube transferred into microfluidic channels, which can only be measured via far-field laser confocal means in visible spectral range [32,33]. To realize the real on- chip optofluidic functionality, it is crucial to demonstrate optofluidic coupling of the microtube cavities integrated onto on-chip waveguides capable of working in the telecom band, which remains unexplored. Fortunately, as discussed in the previous chapter, monolithic integration of VRU-MRRS with nanophotonic waveguides (i.e., Si waveguides) for 3D photonic integration has been successfully reported. It has been shown that resonant filtering of optical signals at telecom wavelengths can be achieved with this intriguing vertical coupling scheme. More importantly, in this work, it is suggested that the fully-integrated system (i.e., VRU-MRRs-waveguides systems) is a breathtaking and crucial platform.

***Corresponding author:** IFW Dresden, Institute for Integrative Nanosciences, Cambridge Graphene Centre, University of Cambridge, Black Semiconductor GmbH,Otto-Blumenthal-Strasse Germany Email-Id: am2692@cam.ac.uk

Received: December 9, 2020 **Accepted:** December 24, 2020 **Published:** December 31, 2020

for optofluidic applications (for more information). Interestingly, in this work, our microtubes are also made from non-toxic biocompatible materials (i.e., TiO2) and can be integrated with several waveguides, which makes them exciting candidates for massively parallel optofluidic detection of diverse analytes. However, optofluidic functionality using this kind of integrated system (i.e., tubular microresonators-waveguides) is not done so far. Thus, this chapter is dedicated to demonstrating optofluidic applications from the fully integrated systems. Two techniques are explored to verify the optofluidic functionality of the system (1) by uniquely filling the hollow core of microtubes with a liquid medium [32] and (2) by fully covering the microtube's surface with a droplet of liquid, which is equivalent to immersing the other microtubes into a liquid medium.

The former case highlight that integrated microtube can be used simultaneously as the sensor heads and also the invaluable microfluidic channels through injection a liquid inside the tube core [33]. In principle, this work reports a simple and less costly method to fabricate large arrays of tubular fluidic channels integrated with on-chip waveguides, which are well-suited for potential biological/chemical sensing and analysis in a lab-on-chip system. In the first part of this chapter, a monolithic integration of large arrays of ultra-compact rolled-up TiO2 microtube vertical optical ring resonators with several polymer waveguides is illustrated, not only to demonstrate the reproducibility and reliability of this intelligent technique but also to present a novel platform for the implementation of optofluidic application.

Next, the physical characterization of these fabricated microtube resonators by optical and scanning electron microscopy are illustrated to highlight the high quality of the fabrication process. The integrated system is compact and mechanically stable to sustain microfluidic environment. The following section of this chapter describes details on the optical confinement of IR light (1,500-1,600 nm) in a microtube with subwavelength wall thicknesses in a situation in which the core of the microtube is initially filled with air and then filled with a liquid medium (purified water). Finally, we consider the case when the outside of the tube is fully covered with a droplet of a liquid (purified water) and is still able to support optical modes. Thus, both methods illustrate a compact, very robust integrated system with the potential to replace today's widespread use of costly photoluminescent spectroscopy and/or complicated fiber-taper coupling schemes [34]. Additionally, the integrated microtubes which their hollow core filled with air have enhanced extinction ratios (ERs) and quality factors as compared to the microtubes investigated. This indicates that the integrated system is nearly in the critical-coupling regime which optical modes possess high ERs.

It is worth noting that there are plenty of novelties in this achievement [32,33]. For example: (1) to date, this is the first experimental realization of optofluidic based free-standing VRU-MRRs suspended in air and seamlessly coupled to on-chip polymer waveguides; (2) in contrast to previous works, this experiment is not bound to the spectral emission range of embedded emitters; (3) the integrated system reduces complexity and improves flexibility; (4) as mentioned before, the integrated system is a good solution for cooling down 3D optoelectronic systems, and this is important because thermal is one of the biggest obstacles to implementation of such systems; (5) most important, due to the compatibility between the processing techniques of VRU-MRRs and microfluidic systems, further chip-level integration of the VRU-MRRs in a microfluidic system is possible, which will be a topic of research for our group in the near future [35]. Broadly speaking, the key innovation of this experiment is creating a fully integrated and portable optofluidic sensor.

Experimental Section: Optical Filter Based on an Optofluidic Micro-Ring Resonator

Fully Integration of an Array of VRU-MRRs with Polymer Waveguides

The fully-integrated VRU-MRRs studied in this work for optofluidic applications, are demonstrated based on our newly developed technique, in which the details can be found in Here, I briefly describe the fabrication process. The process flow for fabrication of the fully integrated sensor mainly consists of three steps. First, a ~2.53 to 2.6 μm thick photoresist (AR-P 3510, Allresist GmbH) is spin-coated onto the photonic chip as a sacrificial layer.

The photonic chip is embedded with polymer waveguides. Note that the polymer waveguides are fabricated from a ~2.5 μm thick SU-8 10 layer (MicroChem, MA, USA; negative photoresist) on a Si substrate coated with a 1.9 μm thick layer of SiO2 using simple photolithography and wet-etching techniques. In this experiment, all fabricated waveguides have a uniform height of 2.5 μm and their widths vary from 3 to 5 μm.

The thickness of the SU-8 layer ensures that the waveguides exhibit single transverse mode operation. Next, standard photolithography is employed to fabricate an array of U-shaped photoresist patterns for rolled-up microtubes preparation. Then, a 115 nm thick layer of differentially strained TiO2 was deposited on the surface using tilted electron beam evaporation. Finally, the photoresist was then dissolved using an organic solvent (Dimethyl sulfoxide) leading to relaxation of the 2D differentially strained nanomembranes which caused them to roll-up into 3D microtube structures over the polymer waveguides. Note that, E-beam lithography was not required because of the vertically coupled configuration of the devices. It is worth mentioning that all of these fabrication steps are completely compatible with standard CMOS planar processing techniques.

Physical Characterization of Polymer Waveguides Coupled TiO2 VRU-M

Figure shows two optical and four SEM images of the VRU-MRRs fabricated in this manner (Figure 6.1). Figure illustrates an overview of an ordered array of fully integrated VRU-MRRs suspended in air and seamlessly overlaid over several integrated waveguides on a single chip (Figure 6.1 (a)). This highlights that monolithic on-chip integration of these VRU-MRRs with polymer waveguides seems straightforward. In Figure details of the VRU-MRR are shown which emphasize the high quality of the fabrication process. The outline of the U-shaped pattern is visible in the background (Figure 6.1(b-f)).

The existence of the legs on both sides of micro tube ensures that there is a vertical gap between the middle part and the waveguide itself. Figure indicates that the smoothness of the tube surface is excellent. The cross-sectional SEM images of the integrated VRUM system were revealed by focused ion-beam (FIB) cutting (Figure 6.1 (d)). Display how the membrane is rolled so tight that the windings are in contact with one other, which produces an ultra-compact microtube wall that is suitable for confining WGMs (Figure 6.1 (d-f)). To protect the tube sample, a carbon layer was coated on top surface of the tube before FIB milling (Figure 6.1 (e)). Moreover, as shown in Figure,

the middle part is elevated above the waveguide with a nanometer gap between them which are well-suited to provide a strong optical coupling from the waveguide to the VRU-MRR and vice versa (Figure 6.1 (f)). The gap can be precisely tuned by controlling the number of turns performed by the rolled-up microtube and changing the thickness of the photoresist. The fabricated VRU-MRRs have a mean diameter of 20 μm, a length of ~200 μm, ~ 4.5 windings in the "thick ends", and ~2.38 windings in the "thin free-standing part" resulting in a wall thickness of about ~274 nm in the middle part. The height of the waveguide is ~2.5 μm and the thickness of the photoresist (i.e. the distance between the tube bottom and the substrate) is between 2.5 and 2.51 μm. Thus, the gap between the middle part of the tube and the waveguide is expected to be between 115 nm and 125 nm (Figure 6.1 (e)). System is nearly in critical-coupling regime in which WGMs have a remarkable ERs which is a higher than our previous achievement (Figure 6.1 (e)).

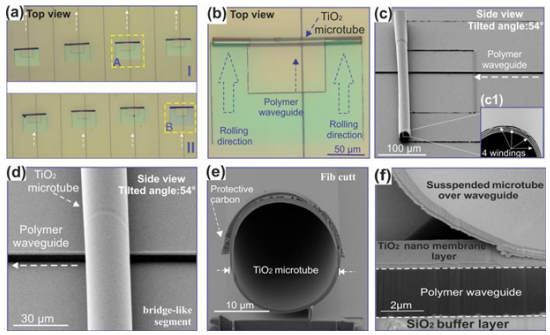

Figure 1: Error! No text of specified style in document. (a) Top view optical microscopy images of an ordered arrays of fully integrated VRU-MRRs spanning over several waveguides on a single chip. These images are taken from two different parts of the same chip (part "I" and part "II"). The transmission results presented in this paper come from the tubes which are indicated with "A" and "B". (b) and (c) show an overview of a single VRU-MRRs vertically coupled to waveguide. (c1) show a magnification of the one end of microtube with very tight rolling and compact windings. (d) A magnification of the center bridge-like part of the VRU-MRRs with an outer diameter of ~20 μm creates. (e) A tilted angle view of the air suspended microtube opening revealing tight, compact windings which highlight the high quality of the fabrication process. windings which highlight the high quality of the fabrication process. Images (e) and (f) are taken after FIB cutting from the upper arm of the tube (see (b) and/or (c)) and the free standing part in the coupling point.

Optical Characterization of the Fully-Integrated System

Optical characterization was accomplished at telecom wavelengths by means of evanescent mode excitation. In this experiment, the transmission setup from was used with one difference. Here, a butt-coupling configuration was performed instead of the vertical coupling scheme. This transmission measurement configuration is illustrated in (Figure 6.2 (a)). Briefly, in this setup, two lensed fibers are horizontally positioned very close to the facet of the waveguide at both ends to couple light in and out of it through the waveguide. The gap between the lensed fibers and the facet of the waveguide is around ~1 μm. Polarized light from a tunable infrared laser (1,500-1,600 nm) was coupled into the waveguide, which was subsequently launched into the VRU-MRR. The light will be coupled into the VRU-MRR to form WGM resonance when its wavelength satisfy the resonant condition, manifesting as sharp intensity drops in the transmission spectrum measured by the point detector. The polarization of the incoming light to be launched into the waveguide was set by a polarization controller that was positioned after the tunable laser (Figure 6.2).

Optofluidic Functionality of the Fully-Integrated Systems

To explore the optofluidic functionality of the on-chip integrated VRUM system, two configurations were investigated to demonstrate the optical response to the presence of liquid. In one configuration, the hollow core of the tube, as a microfluidic channel, was uniquely filled with purified water (refractive index n=1.33) by placing a droplet of the liquid at the bottom end of the tube utilizing a glass capillary and microsyringe [as illustrated in the left panel of figure] while in the other configuration the other surface of the tube is covered by a big droplet of the liquid [as illustrated in the left panel of figure] (Figure 6.3(a),6.4(a)). In the former case, the capillary force was used to rapidly accommodate liquid microdroplets into the core of the microtube. The presence of liquid in the surrounding medium of the microtube results in a change in refractive index and, as a result, leads to spectral shifts of the WGMs. By quantifying these shifts, the sensitivity of the tube to change in a fluid refractive index was determined by using (, – ,)/(–), where , and , are the resonant mode m with and without liquid while and are the refractive indices of the liquid and air, respectively. Here it should be remarked that for perfect optofluidic lab-on-a-chip applications, additional integration processing for pumping liquid into and out of the tube is indispensable. This will be the subject of future studies (Figure 6.3).

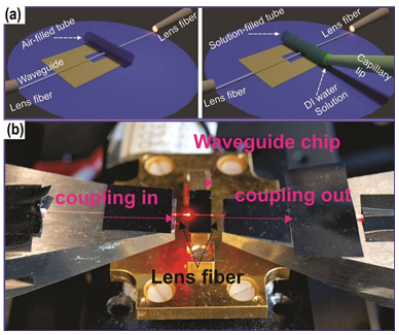

Figure 2: Error! No text of specified style in document. (a) Schematic illustration of the fiber butt-coupling set-up for measuring the transmission spectra of the integrated tube resonator; from the air-filled tube (left-panel) and/or when integrated with solution-filled tubes for optofluidic detection (right-panel). (b) An optical images of the used the setup in this experiment.

Optical Modes in Fully-Integrated VRU-MRRs When the Tube Core is Filled with a Liquid Medium

A representative (but more or less arbitrarily chosen) tube-A shown in figure is selected to fill in purified water, which is pumped from a capillary tip relying on capillary force (Figure 6.1(e)). Here, two measured transmission spectra of optical waveguides coupled to this tube is reported, in the case of the hollow core of the tube filled with air (i.e., empty tube), and then when it is filled with a liquid (Figure 6.3)). In this experiment, the incoming light is polarized parallel to the VRU-MRR axis in the free space.

The transmission spectra with a blue curve correspond to the measurement of an empty (air-filled) VRU- MRR. Owing to the excellent coupling of the signal into the integrated VRU-MRR, a series

of transmission dips (WGMs) are manifested with mode numbers ranging from m = 60 to 65. These mode numbers are simply identified by 2D simulations and marked with blue triangles [Maps of the electric field intensity for mode m=60 WGM for air-filled VRU-MRRs is given in the upper panel .The major optical modes appear at 1515.08 nm, 1531.59 nm, 1548.82 nm, 1565.73 nm, 1582.67 nm, and 1599.82 nm with an ER as high as 23 dB at 1582.67 nm. These wavelengths are in agreement with WGM resonant condition in the VRU-MRR and their FSRs (16.5 nm) agrees very well with the theoretical calculation. Here the quality (Q) factor of the resonant mode was measured up to 500 at λ = 1582.67 nm, allowing for a fine measurement of the spectral shift. When the hollow core of VRU-MRR "A" was uniquely filled with purified water (n=1.33), an analogous series of transmission dips (WGMs) were still observed but the positions of the spectral dip shifted significantly to the longer wavelengths (red-shifte resonant modes are shown in (Figure 6.3)). This can be attributed to the change in the refractive index of the tube core (change from nair=1 to nliquid =1.33) caused by the present of new medium, as shown with a red in (Figure 6.3 (a)). Similarly, the peak positions of the solution-filled can be reproduced by a FDTD simulation (see red triangular markers in the associated electric field intensity maps in the bottom-panel of Figure (Figure 6.3 (a,b)). The WGM field profiles are clearly shown and it is obvious that the evanescent wave penetrates more deeply into the inner part of the tube and that WGMs shift compared to the air-filled micro tube in figure.

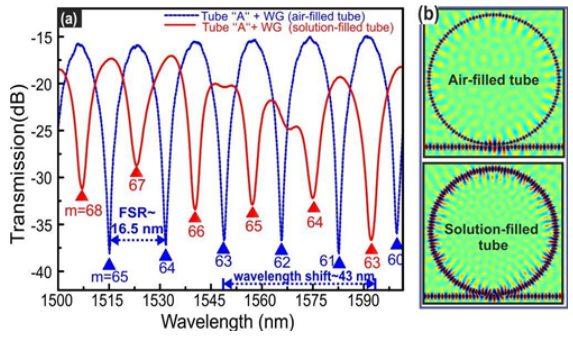

Figure 3: Error! No text of specified style in document. (a) Transmission measurements of the VRU-MRR "A" (as defined in Figure 1(a)) (i) when the tube initially filled with air (blue curve) and (ii) then the core of tube filled with purified water (red curve) utilizing capillary forces. The liquid forces the resonant modes to shift to longer wavelengths (□□□□□□~43 nm). Calculated mode positions for "m= 60 to 65" (initially filled with air) and for "m=63 to 68" (filled with purified water) are marked by the blue and red triangles, respectively. The transmission spectrum of filled-micro tube with purified water showing the change in extinction ratio and line width owing to the absorption loss increases (b) 2D simulation of optical coupling between waveguide and tube at both situations; the tube filled with air and then with a liquid. In the presence of solution, an enhancement of the electric field spread into the tube core is clear.

By the following the above-mentioned formula, the sensitivity of 130 nm/RIU where RIU denotes refractive index unit is obtained from the integrated system. However, the obtained sensitivity is smaller than what is reported in the previous demonstration with the isolated microtube (i.e., it is not coupled to a waveguide), but it is comparable to liquid core optical ring resonator (LCORR) microsphere, and planar ring resonator sensor. The system fabrication and the optofluidic demonstration pave the way for sensing diverse analytes of picoliter volume in a compact integrated optofluidic system. In addition, after filling in purified water an unavoidable decrease of the extinction ratio (decreased from 23 dB to 10 dB) and Q-factor (decreased from ~500 to ~250) were observed owing to the optical absorption loss to liquid medium (Figure 6.4).

Optical Modes in Fully-Integrated VRU-MRRs Covered with a Liquid Medium

The water droplet covered at the outer surface of VRU-MRR is also investigated to demonstrate the optofluidic response, as schematically shown in (Figure. 6.4(a)). Since a heavier optical loss will occur in this configuration, a VRU-MRR "B" [as defined in Figure] exhibiting a larger extinction ratio (32 dB) is used for the measurement (Figure 6.1 (a)). The two transmission spectra, including six resonant modes, are recorded for optical waveguides coupled to VRU-MRR "B", when the tube is initially filled with air and/or the outside of the tube is fully covered with a droplet of purified water. The transmission spectra with the black curve shown in corresponds to the measurement of an empty microtube "B" (i.e., filled with air). It can be observed that in comparison to the measured transmission spectra of microtube "A", that these two transmissions exhibit very similar resonant modes with a spectral variation of WGM peak positions of less than 1nm which implies reliability and repeatability of our integrated scheme (Figure 6.4 (b)). The transmission spectra with the purple curve shown in figure correspond to the measurement of an integrated microtube covered with droplets of purified water (Figure 6.4 (b)). Note that, a mode (m=63) shift of 46 nm is observed. By the following aforementioned formula, the sensitivity of this tube is calculated to be 140 nm/ RIU which is slightly higher than which are larger than those measured from tube-A.

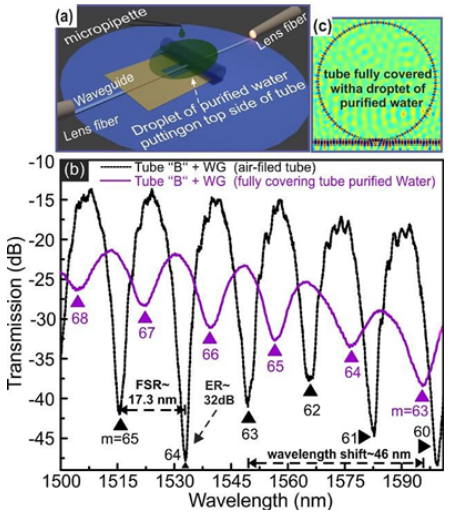

Figure 4: Error! No text of specified style in document. (a) Schematic demonstration of the setup for measuring the transmission spectra of the tube "B" resonator when is fully covered with a droplet of purified water. (b) Transmission measurements of the tube "B" (as defined in figure. 1 (a)) (i) when the tube initially filled with air (black curve) and (ii) when the outside of tube fully covered with a droplet of purified water (purple curve).The liquid causes the resonant modes to shift to longer wavelengths (□□□□□□~ 46 nm). Calculated mode positions for "m= 60 to 65" (filled tube with air) and for "m=63 to 68" (tube immersed into water) are marked by the black and purple triangle, respectively. The transmission spectrum of covered microtube with water droplet showing the change in extinction ratio and linewidth owing to the absorption loss increases (c) 2D simulation of optical coupling between waveguide and tube which is fully covered with a droplet of a purified water droplet. This experiment shows the robustness of our integrated devices.

This increase is caused by a more pronounced penetration of evanescent field in the outer medium of the tube, compared to that in the inner medium. The sensitivity presented in this work is not at the same level of the best results demonstrated previously by our groups and others [33]. Note that by fabricating microtube resonators with a thinner wall thickness and reducing the absorption in the liquids with detecting lightin the visible range, the VRU-MRR-based sensor can potentially offer much greater sensitivity. However, it is expected that there is enough room for improving the sensitivity of our integrated sensor. Interestingly, in contrast with silica based resonators, the capability of these VRU-MRR based TiO2 to support WGM immersed in water is momentous for many potential applications such as bio-sensing, photo-catalysis and dye-sensitized solar cells. Additionally, after a water droplet covering, one can see in the extinction ratio decreases from 32 dB to 10 dB and the Q-factor drops to ~50 owing to the heavy optical loss in the water-covering configuration. In the end, it should be noted that additional transmission measurements are performed over other VRU-MRR-waveguide systems exhibiting similar results as presented in, which indicate an excellent wafer-scale mass fabrication of VRU-MRRs vertically suspended over many waveguides (Figure 6.3 (a)). More importantly, it worth also mentioning that all transmission measurements (with and without a liquid medium) were done a few times to prove the repeatability of our work. (Figure 6.4 (b)).

Conclusion

In conclusion, arrays of ultra-compact 3D microtubular vertical optical ring resonators have been monolithically integrated onto on-chip polymer waveguides. Optical transmission measurements of the integrated system reveal remarkable extinction ratios up to 32 dB, indicating an excellent optical coupling between the vertical tube resonators and the waveguides. To date, this is the highest values reported for VRU-MRRs. Optofluidic functionality is demonstrated by determination the spectral shifts of the resonance modes when the hollow core of the tube is filled and or the outside of the tubes are covered with a liquid droplet. This study represents an intriguing vertical coupling scheme that achieves not only resonant filtering of optical signals at telecom wavelengths but also analyzes the possibility using them as a novel platform for optofluidic biological/chemical detection and analysis in extremely small analyte volume.

References

1. Armani AM, Kulkarni RP, Fraser SE, Flagan RC,Vahala KJ (2007) Label-free, single molecule detection with optical microcavities. Science 317: 783-787.
2. Vollmer F, Yang L (2012) Review label-free detection with high-Q microcavities: a review of biosensing mechanisms for integrated devices. Nanophotonics 1: 267-291.
3. Kipp T, Welsch H, Strelow Ch, Heyn Ch, Heitmann D (2006) Optical modes in semiconductor microtube ring resonators. Phys Rev Lett 96: 077403.
4. Songmuang R, Rastelli A, Mendach S, Schmidt OG (2007) From rolled-up Si microtubes to SiOx/Si optical ring resonators. Appl Phys Lett 90: 091905.
5. Bernardi A, Kiravittaya S, Rastelli A, Songmunag R, Thurmer DJ, et al. (2008) On-chip Si/SiOx microtube refractometer. Appl Phys Lett 93: 094106.
6. Harazim SM, Bolanos Quinones VA, Kiravittaya S, Sanchez S, Schmidt OG (2012) Lab- in-a tube: on-chip integration of glass optofluidic ring resonators for label-free sensing applications. Lab Chip 12: 2649-2655.
7. Renfer A, Tiwari MK, Tiwari R, Alfieri F, Brunschwiler T (2013) Microvortex-enhanced heat transfer in 3D-integrated liquid cooling of electronic chip stacks. Int J Heat Mass Transf 65: 33-43.
8. Vollmer F, Arnold S (2008) Whispering-gallery-mode biosensing: label-free detection down to single molecules. Nat Methods 5: 591-596.
9. White IM, Oveys H, Fan X (2006) Liquid-core optical ring-resonator sensors. Optics Letters 31: 1319.
10. Pöllinger M, Shea DO, Warken F, Rauschenbeutel A (2009) Ultrahigh-Q tunable whispering-gallery-mode microresonator. Phys Rev Lett 103: 053901.
11. Tian Z, Veerasubramanian V, Bianucci P, Mukherjee S, Mi Z, et al. (2011) Single rolled-up InGaAs/GaAs quantum dot microtubes integrated with silicon-on- insulator waveguides. Optics Express 19: 12164-12171.
12. Böttner S, Li S, Trommer J, Kiravittaya S, Schmidt OG (2012) Sharp whispering-gallery modes in rolled-up vertical SiO2 microcavities with quality factros exceeding 5000. Optics Letters 37: 5136-5138.
13. Smith EJ, Xi W, Makarov D, Mönch I, Harazim S, et al. Lab-in-a-tube: ultracompact components for on-chip capture and detection of individual micro-/nanoorganisms. Lab Chip 12: 1917-1931.
14. Strelow Ch, Kietzmann S, Schramm A, Seher R, Hakkarainen T, et al. (2012) AlInP-based rolled-up microtube resonators with colloidal nanocrystals operating in the visible spectral range. Appl Phys Lett 101: 113114.
15. Miao SD, Chen D, Madani A, Jorgensen MR, Bolaños Quiñones VB, et al. (2014) Optofluidic sensor: evaporation kinetics detection of solvents dissolved with Cd3P2 colloidal quantum dots in a rolled-up micro-tube Advanced. Optical Material 3: 187-193.
16.
17. Strelow C, Rehberg C, Schultz CM, Welsch H, Heyn C, et al. (2008) Optical microcavities formed by semiconductor microtubes using a bottlelike geometry. Phys Rev Lett 10: 127403.
18. Mei Y, Huang G, Solovev A A, Ureña EB, Mönch I, et al. (2008) Versatile approach for integrative and gunctionalized tubes by strain engineering of nanomembranes on polymers. Advanced Material 20: 4085-4090.
19. Bolaños Quiñones VA (2015) Rolled-up microtubular cavities towards three-dimensional optical confinement for optouidic microsystems.
20. Madani A, Böttner S, Jorgensen MR, Schmidt OG (2014) Rolled-up TiO2 optical microcavities for telecom and visible photonics. Optics Letters 39: 189-192.
21. Madani A, Kleinert M, Stolarek D, Zimmermann L, Schmidt OG (2015) Vertical optical ring resonators fully integrated with nanophotonic waveguides on silicon-on- insulator substrates. Optics Letters 40: 3826-3829.
22. Bolaños Quiñones VA, Huang GS, Plumhof JD, Kiravittaya S, Rastelli A, et al. (2009) Optical resonance tuning and polarization of thin-walled tubular microcavities. Optics Letters 34: 2345-2347.
23. Huang GS, Bolaños Quiñones VA, Ding F, Kiravittaya S, Mei YF, et al. (2010) Rolled-up optical microcavities with subwavelength wall thicknesses for enhanced liquid sensing applications. ACS Nano 4: 3123-3130.
24. Bolaños Quiñones VA, Ma LB, Jorgensen MR, Kiravittaya S, Schmidt OG, et al. (2012) Localized optical resonances in low refractive index rolled-up microtube cavity for liquid core optofluidic detection. Applied Physics Letters 101: 151107.
25. Psaltis D, Quake SR, Yang Ch (2006) Developing optofluidic technology through the fusion of microfluidics and optics. Nature 442: 381-386.
26. Armani AM, Armani DK, Min B, Vahala KJ, Spillane SM (2005) Ultra-high-Q microcavity operation in H2O and D2O. Appl Phys Lett 87: 151118.

27. Levy U, Campbell K, Groisman A, Mookherjea S, Fainman Y (2006) On-chip microfluidic tuning of an optical microring resonator. Appl Phys Lett 88: 111107.

28. Foreman MR, Swaim JD, Vollmer F (2015) Whispering gallery mode sensors. Adv Opt Photon 7: 168-240.

29. Zamora V, Díez A, Andrés MV, Gimeno B (2007) Refractometric sensor based on whispering gallery modes of thin capillaries. Optics Express 15: 12011-12016.

30. Robinson JT, Chen L, Lipson M (2008) On-chip gas detection in silicon optical microcavities. Optics Express 16: 4296-4301.

31. Hanumegowda NM, Stica CJ, Pate BC, White IM, Fan X (2005) Refractometric sensors based on microsphere resonators. Appl Phys Lett 87: 201107.

32. White IM, Zhu H, Suter JD, Hanumegowda NM, Oveys H, et al. (2007) Refractometric sensors for lab-on-a-chip based on optical ring resonators. IEEE Sensors Journal 7: 28-35.

33. Sumetsky M, Windeler RS, Dulashko Y, Fan X (2007) Optical liquid ring resonator sensor. Optics Express 15: 14376-14381.

34. White IM, Zhu H, Suter JD, Fan X, Zourob M (2009) Label-free detection with the liquid core optical ring resonator sensing platform. Methods Mol Biol 503:139-165.

35. Fan X, White IM, Zhu H, Suter J, Oveys H (2007) Towards lab-on-a-chip sensors with liquid-core optical ring resonators.

36. White IM, Oveys H, Fan X, Smith TL, Zhang J (2007) Demonstration of a liquid core optical ring resonator sensor coupled with an ARROW waveguide array. 6475- 6pp.